Optics Letters

# Model-free deflectometry for freeform optics measurement using an iterative reconstruction technique

Logan R. Graves,[1] Heejoo Choi,[1] Wenchuan Zhao,[2] Chang Jin Oh,[1] Peng Su,[3] Tianquan Su,[4] and Dae Wook Kim[1,5,*]

[1]College of Optical Sciences, University of Arizona, 1630 E. University Blvd., Tucson, Arizona 85721, USA
[2]The Institute of Optics and Electronics, Chinese Academy of Sciences, Chengdu 610209, China
[3]ASML Corporation, 77 Danbury Road, Wilton, Connecticut 06897, USA
[4]KLA-Tencor Corporation, 3 Technology Dr., Miltipas, California 95035, USA
[5]Steward Observatory, University of Arizona, 933 N. Cherry Ave., Tucson, Arizona 85719, USA
*Corresponding author: letter2dwk@hotmail.com

Received 26 February 2018; revised 27 March 2018; accepted 29 March 2018; posted 30 March 2018 (Doc. ID 324660); published 26 April 2018

**We present a novel model-free iterative data-processing approach that improves surface reconstruction accuracy for deflectometry tests of unknown surfaces. This new processing method iteratively reconstructs the surface, leading to reduced error in the final reconstructed surface. The method was implemented in a deflectometry system, and a freeform surface was tested and compared to interferometric test results. The reconstructed departure from interferometric results was reduced from 15.80 μm RMS with model-based deflectometry down to 5.20 μm RMS with the iterative technique reported here.** 

***OCIS codes:*** (120.0120) Instrumentation, measurement, and metrology; (120.6650) Surface measurements, figure; (120.4640) Optical instruments.

https://doi.org/10.1364/OL.43.002110

With ever-growing improvements in freeform optical fabrication, there is a high demand for accurate and dynamic metrology systems. Deflectometry and interferometry are two popular optical test methods that provide high accuracy surface metrology of a unit under test (UUT) [1,2]. Interferometric testing requires a null setup to obtain accurate results. For testing freeform surfaces or highly aspheric surfaces, the interferometer requires a null-optic, such as a computer-generated hologram (CGH) [3]. However, such null optics can be expensive and only work for one configuration.

Deflectometry is a non-null test method that has been shown to provide surface reconstruction accuracy similar to commercial interferometric systems for spherical, aspheric, and off-axis optics [4–6]. The measurable UUT surface area and slope range, referred to as the dynamic range, directly depend on the system hardware configuration. A deflectometry system uses a source which illuminates a UUT and the reflected rays are recorded by a camera. If a clear line of sight can be made from a camera pixel to the UUT surface area (mapped on the camera detector) to a point within the source area (limited by source extent), obeying the law of reflection, it is within the testable dynamic range of the system. The outputs of a deflectometry test are the coordinates of the source which illuminate each camera detector pixel. To process the data, every camera pixel has a ray traced along its pointing vector to an intercept point at the UUT model. The local slope at the intercept point required to send the ray to the recorded source point is calculated. The local slopes are integrated to reconstruct the UUT surface. Any error in the ray coordinates directly affects the reconstruction accuracy. Hardware and calibration approaches allow for error mitigation in detector and source coordinates [5,6]. An error in calculated UUT intercept coordinates is controlled by having an accurate UUT model to trace to. Unfortunately, there are times when the model is not well known, such as during the grinding phase of an optic, where the root-mean-square (RMS) surface shape error from ideal changes from the millimeter-to-micron scale. Without an accurate surface model, it is nearly impossible to correctly determine the ray intercept coordinates at the UUT surface, leading to errors in the reconstructed surface. It is worth noting that low-spatial to mid-spatial frequencies are particularly suspect, as they often represent the largest magnitude error between the UUT model and reality [5].

Reconstruction methods, when no accurate UUT model exists, are limited, and they require a user input surface model. One approach is to assume a flat for the UUT model, which works well for flat UUTs or near-flat UUTs. Proper calibration is required for accurate deflectometry reconstruction. Using an iterative system parameter optimization process leads to improved reconstruction results [7]. A rapid reconstruction method using a non-zonal parameter dependent integration to improve the initial UUT model, followed by a successive over-relaxation zonal integration can improve reconstruction, provided the initial surface model is accurate enough [8,9].

All methods described are user input intensive, however. Extending preliminary work [10], which required a seed input surface model and was only used for a spherical UUT, we have created a general iterative data-processing technique that removes the need for an input surface model, known as model-free iterative deflectometry (MID). It improves reconstruction of freeform surfaces, including the low spatial frequency terms which could not be accurately reconstructed using the previous non-iterative techniques. The MID approach takes no input UUT model; instead, it utilizes the freeform-reconstructed surface that is the output from a deflectometry measurement as a continuously updating surface model for the UUT. This process is repeated until the reconstructed surface converges. The feature of adjusting all spatial frequencies, including the low order shape, which often contains the largest discrepancy between the initial guess (i.e., flat) and the true shape of the UUT model at each iteration, allows for improved reconstruction accuracy across all spatial frequencies. In this Letter, we present reconstruction results from data collected via a software configurable optical test system (SCOTS) [5], which demonstrate the improved performance the MID technique has over traditional non-iterative deflectometry techniques for model-free measurements. Figure 1 illustrates the iterative process and the error an incorrect surface model imparts.

In the MID technique, the Cartesian coordinates in the object space (UUT) of the camera pixels and the source coordinates, defined as matrices $C$ and $S$, respectively, must be known. The UUT surface is unknown, and thus a flat surface model is used, defined as the matrix $U^0$. To bound the solution space, a physical coordinate on the UUT, $u_k(x, y, z)$, must be measured and used in the definition of the UUT surface model. Finally, the ray-pointing vectors of the camera pixels, defined as matrix $R$, are determined via a calibration process. These are the fundamental inputs into the MID process. With these inputs, the MID process runs for $t = 0{:}N$ iterations.

A Delaunay triangulation [11] segments the UUT model into surface planes, defined as matrix $Q^t$, and the intercept locations, defined as matrix $I^t$, are calculated with a Möller–Trumbore algorithm [12]. This combined Delaunay/Möller–Trumbore (DMT) process is a key step in the MID method. The Delaunay triangulation takes the discrete surface points, defined by mapping the camera pixels to the UUT surface, and creates unique planes that are well-shaped triangles and have a nearest-neighbor relation. The number of planes is dependent upon the number of camera pixels. The Möller–Trumbore algorithm, meanwhile, is a rapid 3D ray-triangle intersection method, which calculates the intercept coordinate every camera pixel ray makes with the segmented surface planes via a matrix approach. Processing time for the combined DMT process linearly increases while an improvement in reconstruction accuracy exponentially decays with respect to the number of camera pixels. Figure 2 demonstrates the combined DMT process.

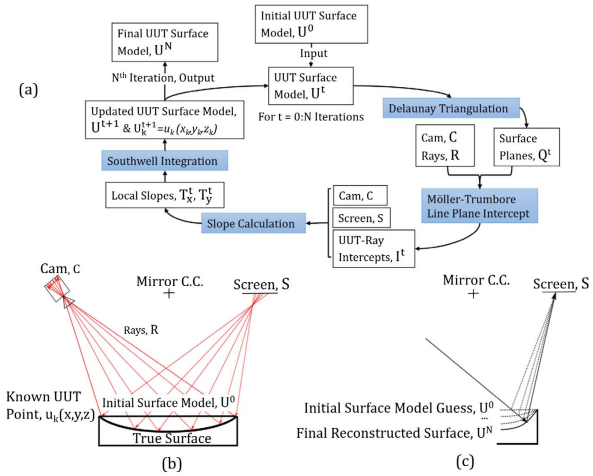


**Fig. 1.** Starting with a surface model guess of $U^0$, the MID process iterates a total of $N$ times to output the final reconstructed surface model $U^N$ (a). Without MID, the rays are traced to the incorrect theoretical surface $U^0$ (b). Using the MID method, the true surface can be converged upon (c).

Using the intercept locations along with the ray start and end points, from $C$ and $S$, the local surface slopes of the UUT in the $x$ direction and the $y$ direction, defined as matrix $T_x^t$ and matrix $T_y^t$, respectively, are calculated. The slopes are integrated using Southwell integration [13] to reconstruct the surface model. This process is iterated, outputting a new reconstructed surface model $U^t$, for a total of $N$ iterations. The final output is the reconstructed surface model $U^N$.

As a numerical verification of the concept, a deflectometry simulation of a known optical surface was performed, and the surface was reconstructed using the MID method. The simulation modeled testing of a UUT with a SCOTS system. The raw deflectometry data, defined as the camera pixel coordinates, the pixel ray directions, the corresponding illuminating screen pixel coordinates for the camera pixels, and a known coordinate on the UUT, were recorded from the simulation. The simulated UUT was one of the hexagonal segments of the James Webb Space Telescope (JWST) primary, a segmented mirror system which uses hexagonal sub-mirrors to make the primary mirror [14]. The segment was 1320 mm in diameter, with a radius of curvature of 15899.91 mm and a conic of –0.99666. The mirror segment was 1320 mm off axis from center. The surface was reconstructed using the MID method for a total of nine iterations. The camera was modeled with $101 \times 101$ pixels, and each iteration took approximately 22.01 s. For the simulation, with an ideal system, the final surface RMS difference from the ideal was 6.17 picometers. With zero iterations, the RMS difference from the ideal was 280.97 μm, thus we see a dramatic improvement in reconstruction accuracy from the MID technique.

To demonstrate the numerical robustness of the MID method against noise, two cases were examined. In the first case, white noise from 0 μm to 1 μm in the $x$ position and the $y$ position was added to the detector coordinates. In the second case, inaccurate global positions of the camera and screen were simulated, with a shift in the position of all camera pixels by 1 mm in the $x$ direction being imparted. Again, nine iterations were used for the MID reconstruction. The final error in the reconstructed surfaces is shown in Fig. 3.

The numerical simulation results suggest that white noise adds a random high spatial frequency error to the reconstructed

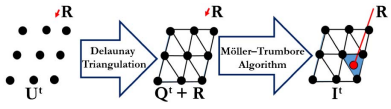


**Fig. 2.** Delaunay algorithm segments $U^t$ into planes, $Q^t$, and the ray ($R$) intercept points $I^t$ are calculated using a Möller–Trumbore algorithm.

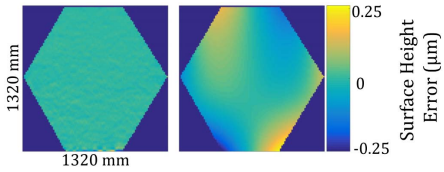


**Fig. 3.** Simulated error from white noise (left) and global positioning error (right) led to an RMS surface error of 11.17 nm and 66.24 nm, respectively, in the final reconstructed surface map.

surface map, with a root mean square (RMS) error of 11.17 nm. Such noise is unavoidable when using common detectors and monitors. The geometric uncertainty error added low spatial frequency error to the final reconstructed map, primarily in the form of astigmatism and coma. Across the reconstructed hexagonal mirror, the RMS error was 66.24 nm and 519.54 nm peak to valley (PV). This error is challenging to reduce without moving to advanced hardware and calibration techniques.

To verify the performance of the MID method in a real measurement, a bare glass optical surface with freeform departure in all directions was manufactured and measured. The radius of curvature (RoC) of the surface was 200 mm, and the diameter was 100 mm. The UUT had a ∼0.67-μm RMS and a ∼2.50-μm PV departure from the base sphere, with a maximum surface slope of 576.64 μrad. The optic was fabricated by Optimax Systems using the magnetorheological finishing (MRF) technique to impart a spiral pattern on the optical surface. The surface was measured with a commercial interferometer, the Zygo Verifire MST, and a SCOTS deflectometry system. A Zygo F/1.75 reference sphere was used as the reference optic for the interferometer. The interferometric technique used does not allow for the accurate reconstruction of the piston, tip, tilt, or power terms of the UUT, and thus they were not analyzed in the deflectometry measurement. Figure 4 demonstrates the complex fringe pattern recorded at the best null condition and the challenges associated with high fringe density in the interferometric test.

For the deflectometry system, a custom SCOTS type system built from off the shelf components was used. We utilized a Point Grey (Model # FL3-U3-32S2M-CS) camera, with a 2.5-μm pixel pitch, due to ease of access to technical specifications. When selecting the monitor, the primary consideration was required source extent to allow for testing the dynamic range of the UUT, which can be described by the aberrated spot size through an inverse ray-tracing from the pinhole location to the UUT, and to the screen. A $7'' \times 5.25''$ Mimo (Model # UM-760F) screen with a 150-μm pixel pitch was selected as it met the dynamic range requirements.

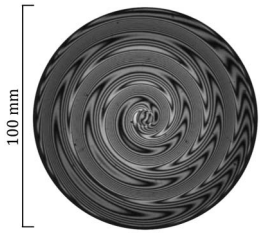


**Fig. 4.** Spiral shape on the UUT made obtaining an interferometric null configuration impossible for the entire mirror. Low modulation due to fringe density led to areas on the surface being unmeasurable.

To calibrate the system and determine the pointing vectors of the camera pixels, a previously described calibration method was utilized [10]. A screen was placed at two positions—$l_1(x,y,z)$ and $l_2(x,y,z)$. The camera was at a fixed position $c(x,y,z)$, and the coordinates of the illuminating screen pixel at $l_1(x,y,z)$ and $l_2(x,y,z)$ for every camera pixel were measured. The ray path for every camera pixel was then calculated. All the coordinates were measured with a coordinate measurement machine (CMM), accurate to ±10 μm.

For the deflectometry test, the UUT was placed on a rotation stage below the screen and camera. All components were mounted in place on a breadboard to maintain position throughout testing. A CMM, accurate to ±10 μm, was used to locate the body edges of the camera and screen using a touch tip. A plane was fit to the screen, while technical drawings relating the camera detector to the body were used to determine the detector coordinates. Additionally, the center point of the UUT, about which it rotated, was located. This served as the known coordinate, $u_k(x_k,y_k,z_k)$ and as the global zero coordinate in $x$, $y$, and $z$. This was related to the camera pixel measuring the known coordinate, pixel $p(x,y,z)$. A phase-shifting deflectometry measurement was then performed. The resulting raw data was recorded for processing.

The raw data was processed in three ways. First, the MID technique was used for a total of six iterations. Also, in a traditional non-iterative way, the data was reconstructed by assuming (1) a flat for the base surface and (2) a 200-mm RoC base sphere model, representing an unknown and known model case, respectively. The same raw data was used for all cases. To account for systematic error in the measurements a rotation calibration was performed [15]. The average error map was determined by reconstructing the UUT measured every 10° for a full rotation and calculating the average, which was subtracted from the final reconstructed map. The reconstructed surfaces generated with the MID technique and the two traditional techniques, referred to as $\text{MID}_6$, $\text{MB}_{\text{flat}}$, and $\text{MB}_{\text{sphere}}$, respectively, were then analyzed to compare the Zernike terms and the reconstructed surface shape to the surface measured by the interferometer, referred to as INT. The missing data regions in the INT are not considered in the comparison, as we did not want to extrapolate/interpolate data for comparison. The surface evolution of the $\text{MID}_6$ through iterations is visualized in Fig. 5.

The Zernike terms were fit to the surfaces and low order spatial frequency terms were analyzed. Table 1 displays the difference from the interferometric result in the low order Zernike terms (RMS normalized) for the $\text{MID}_6$ map, the $\text{MB}_{\text{flat}}$ map, and the $\text{MB}_{\text{sphere}}$ map. The Zernike terms 1–4, the piston, the tip, the tilt, and the power, were removed to match the fact that the interferometer was unable to accurately measure Zernike terms up to Z4. (The interferometric data also

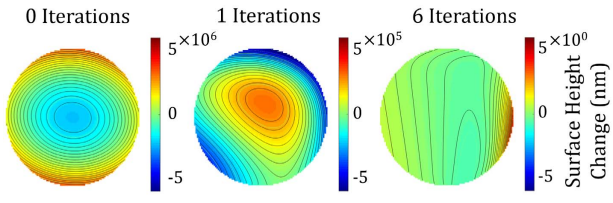


**Fig. 5.** Surface height change between 0 (left), 1 (middle), and 6 (right) iterations shows the most significant change occurs in early iterations. The black lines show the surface contours. (See Visualization 1).

**Table 1. Low Order RMS Normalized Zernike Term Difference between Reconstructed and Interferometric Surface Maps**

| Zernike Term | $MID_6$ (μm) | $MB_{flat}$ (μm) | $MB_{sphere}$ (μm) |
|---|---|---|---|
| Z5, Oblique Astigmatism | 0.76 | 1.90 | 0.42 |
| Z6, Vertical Astigmatism | −5.12 | −44.28 | −15.80 |
| Z7, Vertical Coma | −0.36 | −1.98 | −0.40 |
| Z8, Horizontal Coma | −0.10 | 0.55 | 0.11 |
| Z9, Vertical Trefoil | 0.32 | 1.01 | 0.25 |
| Z10, Oblique Trefoil | −0.05 | 0.29 | 0.06 |
| Z11, Spherical | 0.04 | 0.63 | 0.17 |
| Z5:Z11 Total RMS Diff | 5.20 | 44.39 | 15.80 |

includes its own uncertainties due to high fringe density from the non-null configuration).

The total Zernike term RMS departure, for low order terms Z5–Z11, from the INT for the $MID_6$, $MB_{flat}$, and $MB_{sphere}$ surfaces were 5.20 μm, 44.39 μm, and 15.80 μm, respectively. This demonstrates that without subtracting any low order terms, beyond the standard removal of terms up to power, the MID method provided close to an order of magnitude improvement in accuracy matching the interferometric measurement compared to traditional deflectometry with no accurate model. The reconstructed surface maps, with the increasing Zernike term removal, are shown in Fig. 6.

The MID technique resulted in a surface that more closely matched the interferometric measurement when compared to a traditional non-iterative technique for model-free deflectometry surface reconstruction. Particularly, at the low spatial frequencies, it achieved more similar results to the interferometric measurement. We acknowledge that there are still residual differences, predominantly in the astigmatism and the coma, between the interferometric measurement and the MID reconstructed surface. Small uncertainties in geometrical knowledge of the positions of all components contributed to some of the residual astigmatism and coma in the $MID_6$ reconstructed surface. However, the MID method improves the well-known low order accuracy issues of traditional deflectometry while

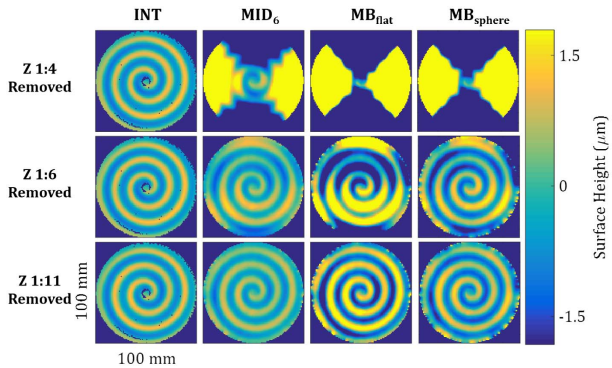


**Fig. 6.** Reconstructed interferometric surface map (first column), MID method with six iterations (second column), and non-iterative traditional reconstruction with a flat UUT model (third column) and a 200 mm RoC base sphere model (fourth column) method had Zernike terms 1–4 (top row), 1–6 (middle row), and 1–11 (bottom row) removed to compare error contribution from low spatial frequency. (Note: excess fringe density led to missing data in the interferometric map).

maintaining the advantage of a large dynamic range, when compared to interferometry. The effect of the dynamic range is particularly clear for this UUT, which suffered from missing data regions in the measured interferometric map due to the inability to obtain a null over the entire surface.

The MID technique represents a novel data-processing solution that can provide more accurate surface reconstruction results for a deflectometry measurement across all spatial frequencies. We do not claim that the MID method is superior to other precision metrology techniques such as interferometry. Instead, we seek only to improve the deflectometry-processing approach to provide more value to the optics metrology community by providing multiple options and crosschecking metrology solutions. The technique is delivered via a software package and can easily be included in an existing deflectometry system's processing pipeline. The MID method seeks only to address the fundamental reconstruction error which arises from inaccurate surface modeling of the UUT. The reported enhancement in measurement accuracy is achieved solely by the new data processing concept, not by improved hardware or calibration techniques. Using the proposed MID method, the same raw data can be reprocessed to produce a higher accuracy result, which was hidden in the raw data but not previously utilized in the surface reconstruction pipeline. This highlights the significance of the MID approach maximizing the use of information in the commonly measured deflectometry data.

**Funding.** II-VI Foundation Block-Gift Program.

**Acknowledgment.** This research was made possible in part by the II-VI Foundation Block-Gift Program, the Technology Research Initiative Fund Optics/Imaging Program, the Freeform Optics project supported by the Korea Basic Science Institute, the Friends of Tucson Optics Endowed Scholarships in Optical Sciences, and we thank Optimax Systems for providing the freeform UUT.

## REFERENCES

1. B. Martin, J. Burge, S. Miller, S. Warner, and C. Zhao, *Frontiers in Optics/OF&T*, OSA Technical Digest (Optical Society of America, 2008), paper OWD6.
2. C. J. Oh, A. Lowman, G. Smith, P. Su, R. Huang, T. Su, D. W. Kim, C. Zhao, P. Zhou, and J. Burge, Proc. SPIE **9912**, 99120O (2016).
3. M. B. Dubin, P. Su, and J. Burge, Proc. SPIE **7426**, 74260S (2009).
4. D. W. Kim, C. J. Oh, A. Lowman, G. Smith, M. Aftab, and J. Burge, Proc. SPIE **9912**, 99120F (2016).
5. R. Huang, *High Precision Optical Surface Metrology Using Deflectometry* (Academic, 2015).
6. D. W. Kim, M. Aftab, H. C. Choi, L. Graves, and I. Trumper, *Frontiers in Optics* (Optical Society of America, 2016), paper FW5G.4.
7. E. Olesch, C. Faber, and G. Häusler, *DGaO Proceedings* (2011), Vol. **112**.
8. T. Zhou, K. Chen, H. Wei, and Y. Li, Appl. Opt. **55**, 2760 (2016).
9. H. Zhang, S. Han, S. Liu, S. Li, L. Ji, and X. Zhang, Appl. Opt. **51**, 7616 (2012).
10. W. Zhao, L. Graves, R. Huang, W. Song, and D. W. Kim, Proc. SPIE **9684**, 96843X (2016).
11. S. Cheng, T. Dey, and J. Shewchuk, *Delaunay Mesh Generation* (CRC Press, 2013).
12. T. Möller and B. Trumbore, J. Graph. Tools **2**, 21 (1997).
13. W. H. Southwell, J. Opt. Soc. Am. **70**, 998 (1980).
14. H. P. Stahl, in *Optical Society of India Symposium: International Conference on Optics and Optoelectronics* (2014).
15. C. Evans, R. Hocken, and W. Estler, CIRP Ann. **45**, 617 (1996).